INTERNATIONAL JOURNAL FOR NUMERICAL AND ANALYTICAL METHODS IN GEOMECHANICS
Int. J. Numer. Anal. Meth. Geomech., **23**, 1159–1170 (1999)

KINEMATIC SLICES APPROACH FOR UPLIFT ANALYSIS OF STRIP FOUNDATIONS

JYANT KUMAR*

Department of Civil Engineering, P.N.G. University of Technology, Private Mail Bag, LAE, Papua, New Guinea

SUMMARY

A kinematic method of slices has been used in this article to deal with the stability problems of strip foundations subjected to uplift loads. The method is based on the upper bound theorem of limit analysis and satisfies the kinematic admissiblility of the chosen collapse mechanism. Assuming the global rupture surface as an arc of logarithmic spiral, uplift factors F_c, F_q and F_γ separately for the effects of cohesion, surcharge and density have been determined. The effect of the yielding of soil mass with partial soil shear strength parameters along the slice interfaces on the results has been examined. The ultimate uplift capacity increases with increase in soil shear strength along the interfaces of slices. The results compare reasonably well with the various existing theories and reported experimental tests data. Copyright © 1999 John Wiley & Sons, Ltd.

KEY WORDS: anchors; failure; foundations; limit analysis; method of slices; soils

INTRODUCTION

Limit equilibrium and limit analysis techniques are widely used to solve various stability problems such as retaining walls, foundations, anchors, embankment slopes, and tunnels. In the limit equilibrium method, only statical global or local equilibrium conditions are employed without considering the kinematics of the problem. The method of characteristics[1] for instance is the rigorous application of the limit equilibrium technique. The method of slices[2–7], another example of the application of the limit equilibrium technique, is often used to deal with stability problems having complicated geometry, non-uniform loading and layered soil media. Limit analysis technique has the advantages of providing rigorous upper and lower bounds with due consideration to the kinematics of the problem. A vast literature[8–12] for obtaining the solutions of various problems using the limit analysis is available at present. Recently, Michalowski[11] has demonstrated the use of the upper bound theorem of limit analysis coupled with the method of slices to determine the stability of embankment slopes. Translational collapse mechanism comprising rigid slices and curved shape of the rupture surface was considered. In the present paper this kinematic method of slices was employed to determine the upper bound solution for the ultimate uplift capacity of foundations. Theoretical estimates for the ultimate uplift capacity of foundations/anchors are available by using the conventional limit equilibrium method (Meyerhof

Correspondence to: Jyant Kumar, Department of Civil Engineering, P.N.G. University of Technology, Private Mail Bag, LAE, Papua, New Guinea

CCC 0363–9061/99/111159–12$17.00

Received 24 September 1997
Revised 23 September 1998

and Adams[13]), the upper bound theorem of limit analysis using linear rupture surfaces (Murray and Geddes[14], Kumar[15]), the finite element method (Rowe and Davis[16–17]) and the method of characteristics (Kumar[18]; Subba Rao and Kumar[19]). The present article provides the uplift factors for the effects of cohesion, surcharge and density. In agreement with the experimental observtions of Meyerhof and Adams[13] and Matsuo[20,21], the shape of the global rupture surface was assumed to be an arc of logarithmic spiral. The effect of yielding of the soil mass with partial soil shear stength parameters along the interfaces of slices on the results has as been investigated. The results obtained from the analysis were compared with various available theories and experimental model tests data of Rowe and Davis[16,17] both in clays and sands.

UPPER BOUND LIMIT ANALYSIS APPROACH

According to the upper bound theorem of limit analysis, the limit load at collapse for any structure can be determined by equating the rate of dissipation of the total internal energy in any kinematic admissible mechanism, to the rate of total work done by external and body forces. For two-dimensional problems, this equality can be expressed mathematically as

$$\int_A \sigma_{ij}\dot{\varepsilon}_{ij}\mathrm{d}A + \int_L t_i[V]_i\,\mathrm{d}L = \int_S t_i V_i \mathrm{d}S + \int_A \gamma_i V_i\,\mathrm{d}A \tag{1}$$

where the first two terms represent the rate of internal work done (dissipation of internal energy) by the stresses σ_{ij} over the strain rates $\dot{\varepsilon}_{ij}$ within region A, and by the tractions t_i over the velocity jump $[V]_i$ along the velocity discontinuity line L. The last two terms define the rate of external work of tractions t_i over velocities V_i along the boundary S, and of body forces γ_i over velocities V_i in region A.

The stresses satisfy the yield condition and are related to the strain rates by the associated flow rule (normality condition):

$$\dot{\varepsilon}_{ij} = \dot{\lambda}\,\partial f(\sigma_{ij})/\partial\sigma_{ij} \tag{2}$$

where $\dot{\varepsilon}_{ij}$ is the strain rate tensor, σ_{ij} is the corresponding stress tensor satisfying the yield condition $f(\sigma_{ij}) = 0$, and $\dot{\lambda}$ is a non-negative plastic multiplier.

The magnitude of limit load obtained from equation (1) is then optimized by trying various possible kinematically admissible rupture mechanisms. The load obtained in this manner provides an *upper bound* on the true limit load inducing collapse (e.g. the magnitude of passive earth pressure and the bearing capacity of foundations), and a *lower bound* on the true limit load resisting the collapse (for instance the magnitude of the active earth pressure). If the material bounded by rupture and boundary surfaces is subdivided into different *rigid* regions undergoing either translation or rotation, the strain rates $\dot{\varepsilon}_{ij}$ within region A will become equal to zero, and equation (1) will become

$$\int_L t_i[V]_i\,\mathrm{d}L = \int_S t_i V_i\,\mathrm{d}S + \int_A \gamma_i V_i\,\mathrm{d}A \tag{3}$$

where the product $t_i[V]_i$ represents the rate of energy dissipation per unit length along the velocity discontinuity/rupture surfaces. For a material obeying Mohr–Coulomb yield condition and associated flow rule, the velocity jump vector $[V]_i$ must incline at an angle ϕ with the velocity discontinuity line; the magnitude of product $t_i[V]_i$ then equals $c[V]_i\cos\phi$.

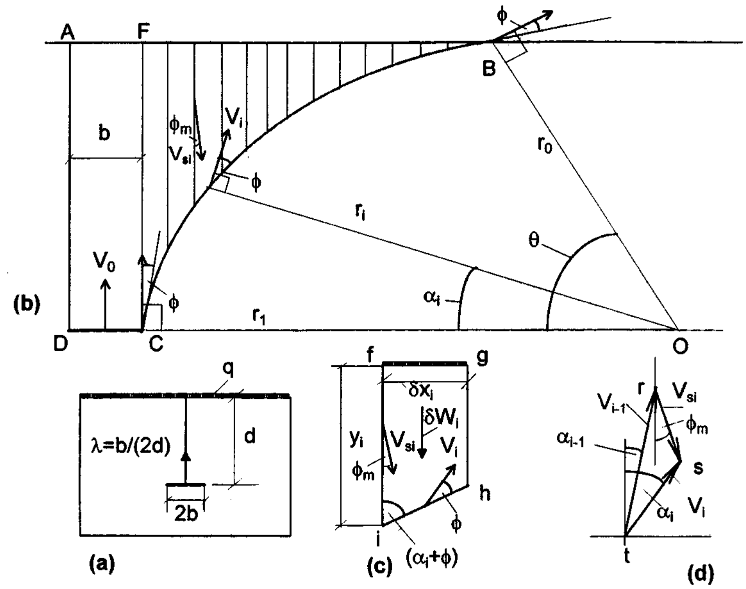

Figure 1. Failure mechanism and velocity hodograph

PROBLEM DEFINITION

A rigid strip anchor of width $2b$, placed at a depth d from the ground is considered. The anchor is subjected to a vertical upward pull as shown in Figure 1(a). The objective of the analysis is to obtain the magnitude of ultimate load P_u at failure.

ASSUMPTIONS

1. The contribution of soil mass below the anchor plate towards the magnitude of P_u, is zero. It will normally be true for anchors/foundations placed at shallow depths and not bonded with the adjoining soil.
2. The global rupture surface is an arc of logarithmic spiral, and it joins the edge of the anchor tangentially to a line inclined at an angle ϕ with the vertical.

Since the tangent at any point on the logarithmic spiral arc makes an angle ϕ with the normal to the corresponding radius vector (radius vector is a line joining any point on the log-spiral and its pole), on the basis of assumption (2), the radius vector joining the edge of the anchor will become horizontal. Accordingly, the pole of the log-spiral arc will always lie on a horizontal line through the edge of anchor.

KINEMATIC METHOD OF SLICES

The conventional methods of slices are based on the assumptions of variation of interslice forces as to satisfy either the two or three conditions of static equilibrium. The kinematic admissibility of

the selected failure mechanism cannot be proven in these methods of slices. The kinematic method of slices can be used by discretizing the soil mass bounded by rupture and boundary surfaces into a number of *rigid* vertical blocks (slices) undergoing translation in a manner shown in Figure 1(b) (see also Michalowski[11]). The actual collapse mechanism for the anchor problem, however, does not show the complete development of plastic zones within the soil mass bounded by rupture and boundary surfaces (see Rowe and Davis[16,17] and Matsuo[20,21]). This means that within the zone which is not plastic, the soil shear strength will not be completely mobilised along the interfaces of different slices. The upper bound theorem of the limit analysis does not require all the soil in the limit state. However, limit state must be reached where plastic deformation is to occur, i.e., it must be reached along the failure surfaces. To extend the use of limit analysis, along the slice interfaces, yielding of soil using partial shear strength parameters c_{m} and ϕ_{m} was assumed to occur. Where $c_{\mathrm{m}} = m \cdot c$; $\phi_{\mathrm{m}} = \tan^{-1}(m \cdot \tan\phi)$; c = cohesion; and ϕ = friction angle of soil, and m is the partial soil strength factor along the interfaces of slices. The value of m will obviously vary in between 0 and 1. For determining the factor of safety of earthen slopes, Karal[22] has already demonstrated the applicability of the limit analysis with the yielding of soil assumed with partial shear strength parameters. However, the analysis with $m < 1$ will provide approximate solutions since the sliding between the slices can occur when the Mohr–Coulomb failure criterion is satisfied, i.e. $m = 1$.

If the soil mass obeys an associated flow rule, the velocity jump vector $[V]$ along the slice interfaces must be inclined at angle ϕ_{m} as shown in Figure 1(c). Consequently, the rate of internal dissipation of energy per unit length along the slice interfaces will become $c_{\mathrm{m}}[V]\cos\phi_{\mathrm{m}}$. However, along the global rupture surface itself the velocity jump vector should be inclined at an angle ϕ.

If the velocity of one block is known, the velocities of all other blocks can be found by constructing the velocity hodographs repeatedly as shown in Figure 1(d). It can be shown that

$$V_i = V_{i-1}\sin(\alpha_{i-1} + \phi_{\mathrm{m}})/\sin(\alpha_i + \phi_{\mathrm{m}}) \tag{4a}$$

$$[V]_{\mathrm{si}} = V_{i-1}\sin(\alpha_i - \alpha_{i-1})/\sin(\alpha_i + \phi_{\mathrm{m}}) \tag{4b}$$

where V_i is the velocity of the ith slice, V_{i-1} the velocity of the $(i-1)$th slice, $[V]_{\mathrm{si}}$ the velocity jump along the interface of the $(i-1)$th and ith slice, α_i the horizontal inclination of the radius vector joining the mid-point of the base of ith slice, and α_{i-1} the corresponding horizontal inclination of the radius vector joining the mid-point of the base of $(i-1)$th slice.

The rate of dissipation of total internal energy along the slice interfaces is given by

$$E_i = \sum_{i=1}^{n+1} y_i[V]_{\mathrm{si}}c_{\mathrm{m}}\cos\phi_{\mathrm{m}} \tag{5}$$

where y_i is the height of ith slice interface, and n the number of slices.

The rate of dissipation of total internal energy along the base of slices is

$$E_{\mathrm{b}} = \sum_{i=1}^{n} V_i c\cos\phi\,\delta x_i/\sin(\alpha_i + \phi) \tag{6}$$

where δx_i is the width of ith slice.

The rate of total work done by the pullout force, body forces and surcharge load,

$$\mathrm{Work} = P_{\mathrm{u}}V_0 - \sum_{i=1}^{n}(\delta W_i + q\delta x_i)V_i\cos\alpha_i \tag{7}$$

where q is the surcharge pressure on the ground surface, V_0 the velocity of anchor, δW_i weight of ith slice $= \gamma \delta x_i y_i$, and y_i the average height of ith slice.

KINEMATICALLY ADMISSIBLE GLOBAL RUPTURE SURFACE

At any point along the ground surface, the soil mass should have positive components of the velocity in the vertical upward direction and in the horizontal direction away from the axis of anchor. To satisfy the latter condition, the minimum angle of intersection of the rupture surface with the ground (horizontal) should be at least equal to $-\phi$. If the angle of inclination of the log-spiral surface with the ground is chosen $-\phi$, the rupture surface emerging from the edge of the anchor will meet the ground surface twice. First, it will intersect the ground surface at an angle $\geqslant 0$, and then will meet the ground again at an angle $-\phi$. This limits the minimum angle of the *first* intersection of rupture surface with the ground equal to zero. Since the pole of log-spiral lies on a horizontal line passing through the edge of anchor, the maximum value of θ, the angle made by the logarithmic spiral arc at its focus O as indicated in Figure 1(b), will become equal to $\pi/2 - \phi$. For any kinematic admissible collapse mechanism, the value of θ, can vary in between 0 and $\pi/2 - \phi$.

For any chosen value of θ, the complete path of rupture surface can be established by making use of the following formulas:

$$r_0 = d/\sin\theta \quad \text{and} \quad r_1 = r_0 \exp(\theta \tan\phi)$$

where r_0 is the initial radius of the logarithmic spiral, and r_1 the final radius of logarithmic spiral arc.

COLLAPSE LOAD

Using the upper bound theorem of limit analysis, the collapse load, P_u can be found from

$$P_u = 1/V_0 \left[\sum_{i=1}^{n} (\delta W_i + q dx_i) V_i \cos\alpha_1 + \sum_{i=1}^{n} V_i c \cos\phi \delta x_i / \sin(\alpha_i + \phi) + \sum_{i=1}^{n+1} [V]_{si} c_m \cos\phi_m y_i \right] \quad (8)$$

A number of different global rupture surfaces can subsequently be tried, to obtain the minimum magnitude of the collapse load.

UPLIFT EQUATIONS

The ultimate uplift pressure, p_u, was expressed in the form of the following equation:

$$p_u - (\gamma d + q) = c\lambda F_c + q\lambda F_q + \gamma(2b)\lambda^2 F_r \quad (9)$$

where $p_u = P_u/(2b \times 1{\cdot}0)$, λ (embedment ratio) $= d/(2b)$, and F_c, F_q and F_γ are the uplift capacity factors for the effects of cohesion, surcharge and unit weight, respectively. By multiplying $2b$ on both the sides, equation (9) can be rewritten in the form

$$P_u - (2\gamma bd + 2qb) = cdF_c + qdF_q + \gamma d^2 F_\gamma \quad (10)$$

Since no discontinuity in the velocity has been allowed (assumption 2) along the vertical line joining the edge of the anchor and ground surface (line CF in Figure 1(b)), the term

$[P_u - (2\gamma bd + 2qb)]$ will represent the component of the failure load entirely due to the resistance offered by the soil wedge FBC against the anchor movement. The geometry of the wedge FBC depends only on the depth of anchor, and is independent of anchor's width. The term $[P_u - (2\gamma bd + 2qb)]$, in a manner like the total magnitude of the backfill force (earth pressure) on retaining walls, will become proportional to d for both the cohesion and surcharge components, and proportional to d^2 for the corresponding unit weight component. The terms associated with F_c and F_q in equation (10) are already proportional to d and that associated with F_γ is proportional to d^2. Therefore, the uplift factors F_c, F_q and F_γ will become independent of the embedment ratio of the anchor (also see Meyerhof and Adams[13]).

RESULTS

Rupture surface and velocity patterns

Computations were performed for each value of m independently in between 0 and 1. It was seen that for $m = 1$, the value of θ, i.e. the angle made by the log-spiral arc at its focus, corresponding to the critical rupture surfaces in all cases becomes almost equal to zero (no curvature of log-spiral). Which implies that the shape of critical rupture surfaces for $m = 1$ becomes almost a straight line (zero curvature). The direction of the resultant velocities everywhere along the rupture surface for $m = 1$ becomes vertical, and their magnitude (for all slices) becomes equal to the velocity of pullout of anchor (V_0). Whereas for values $m < 1$, in all the cases, the value of θ is found greater than zero, i.e. the shape of the critical failure surfaces remains curved. This observation justifies that the value of m should be taken lesser than 1 since in all such cases, the shape of the rupture surface remains curved. The actual experimental observations[13,20,21] and elasto-plastic FEM analysis[16,17] indicate the development of the curved rupture surfaces rather than linear. It was noticed that for $m < 1$, the velocity of slices decreases continuously as the horizontal distance from the axis of the anchor is increased with the positive components in the vertical upward direction and in the horizontal direction away from the axis of anchor.

Variation of the uplift factors F_c, F_q and F_γ

The variation of the uplift factors F_c, F_q and F_γ with ϕ for values of m in between 0 and 1 is indicated in Figures 2–4. All the uplift factors, except the factor F_c with $m = 1$, increase both with increase in ϕ and m. The magnitude of F_c for $m = 1$ becomes equal to 2·0 irrespective of the value of ϕ.

Check for superposition of components in the uplift equation

The division of the anchor capacity into three separate parts, for the effects of cohesion, surcharge and unit weight, assumes that these three components are independent and can be superimposed. Analyses were performed to determine the effect of superposition error for a wide range of the values of ϕ, m, $c/(\gamma d)$ and $q/(\gamma d)$. It was found that the error in assuming superposition was always on the safer side (superposition gives lesser value of P_u than the actual). In all cases the magnitude of error was less than 1 per cent. A comparison of exact and approximate values of failure loads obtained from the principle of superimposition (using equation (9) for

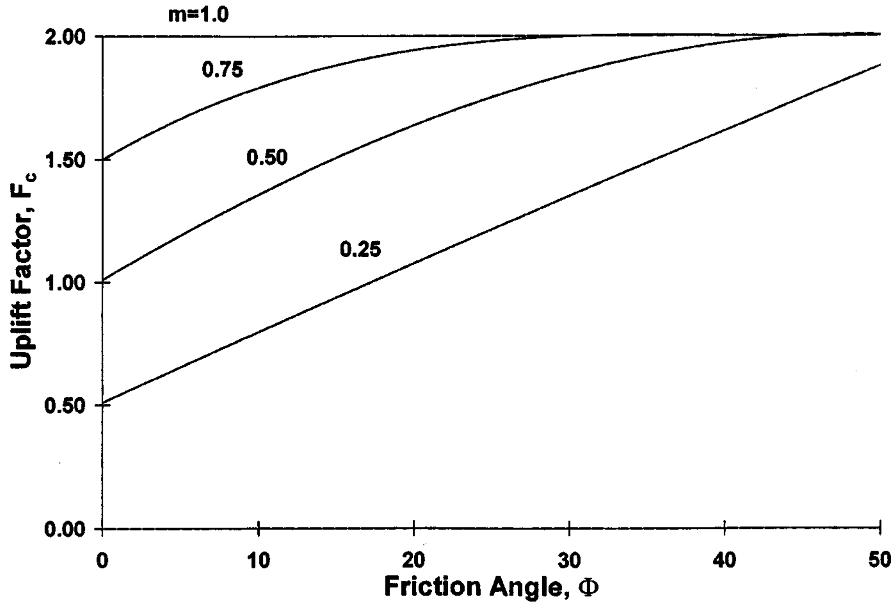

Figure 2. The variation of uplift factor F_c with ϕ and m

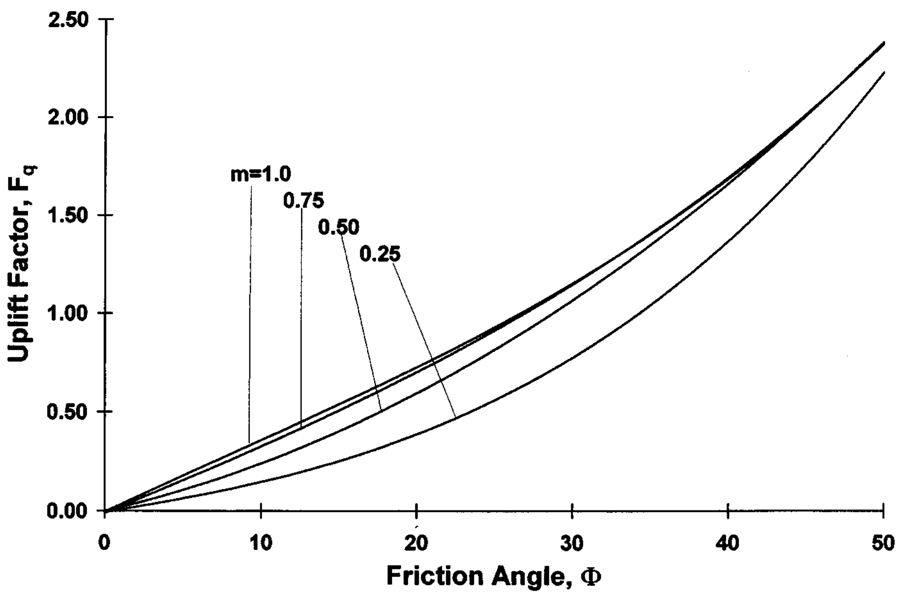

Figure 3. The variation of uplift factor F_q with ϕ and m

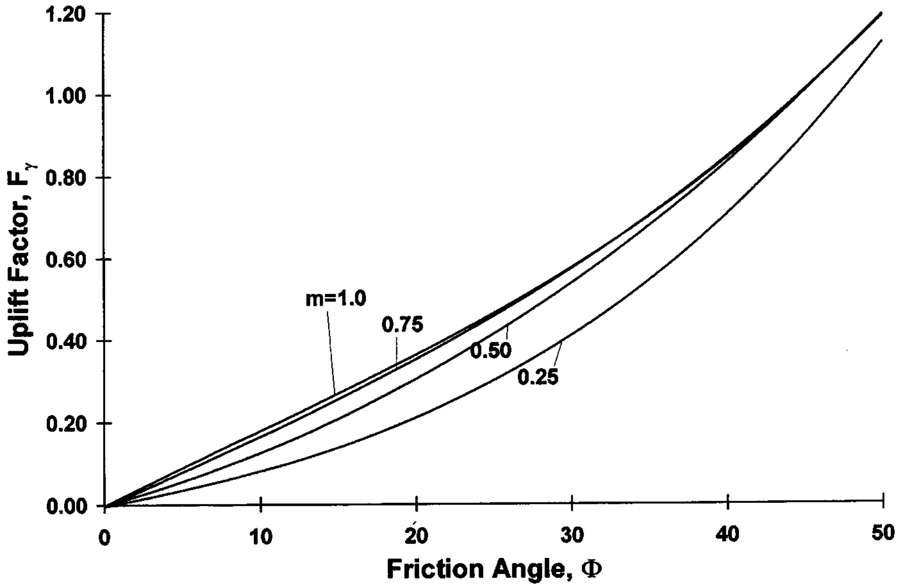

Figure 4. The variation of uplift factor F_γ with ϕ and m

$\gamma = 20{\cdot}0\,\mathrm{kN/m^3}$, $b = 1{\cdot}0\,\mathrm{m}$, $d = 5{\cdot}0\,\mathrm{m}$, $\lambda = 2{\cdot}5$, $\phi = 30°$, $m = 0{\cdot}5$ is shown in Table I. The maximum error is less than 0·1%.

COMPARISONS

With the existing theories

Like the other available theories[13,14,16,17], the kinematic method of slices indicates that the uplift factors F_c, F_q and F_γ increase with the increase in the values of ϕ. The earlier solutions of Murray and Geddes[14] and Kumar[15] based on the kinematic method of limit analysis, but assuming the shape of the global rupture surface as a straight line, produced exactly the same results as given by the present approach for $m = 1$. Both the approaches predict exactly the same vertical inclination of the critical rupture surface, which is equal to ϕ. A comparison of uplift factors F_c, F_q and F_γ with variation in ϕ from the different methods has been shown in Tables II–IV. The finite element approach of Rowe and Davis provides the highest values of the uplift factor F_γ as compared to any other theory. The values of F_q and F_γ from the theory of Meyerhof and Adams lie in between the corresponding values from the present approach for $m = 0{\cdot}5$ and 1·0. The theory of Meyerhof and Adams gives exactly the same values of F_c as given by the present approach for $m = 1{\cdot}0$. For values of ϕ up to around 15° the factor F_c from the Rowe and Davis theory lies in between the corresponding present values for $m = 0{\cdot}5$ and 1·0, whereas for higher ϕ values, Rowe and Davis theory gives lower values of F_c than that obtained from the present approach even for $m = 0{\cdot}5$. In all cases the method of characteristics provides the least values of uplift factors.

Table I. Comparison of exact and approximate values of failure loads obtained from the principle of superimposition (using equation 9) for $\gamma = 20{\cdot}0$ kN/m^3, $b = 1{\cdot}0$ m, $d = 5{\cdot}0$ m, $\lambda = 2{\cdot}5$, $\phi = 30°$, $m = 0{\cdot}5$

$c/(\gamma d)$ $q/(\gamma d)$	0	0·1	1·0	10·0
0	0·46876* 0·46876† 0·000‡	0·56146 0·56097 0·087	1·39,190 1·39,092 0·070	9·69,142 9·69,032 0·011
0·1	0·54234 0·54200 0·063	0·63482 0·63421 0·096	1·46514 1·46,416 0·067	9·76,467 9·76,356 0·011
1·0	1·20,207 1·20,117 0·075	1·29,431 1·29,338 0·014	2·12,435 2·12,332 0·048	10·42,383 10·42,273 0·010
10·0	7·79,392 7·79,283 0·014	7·88,614 7·88,504 0·014	8·71,608 8·71,498 0·013	17·01,549 17·01,439 0·006

* Exact value of failure load (MN/m)·
† The value of failure load (MN/m) from the principle of superimposition (equation 9)
‡ Error in percent

Table II. Comparison of F_c

	Uplift factor, F_c					
ϕ	Meyerhof and Adams [13]	Murray and Geddes [14]	Rowe and Davis [16]	Subba Rao and Kumar [19]	Present analysis, $m = 0{\cdot}5$	Present analysis, $m = 1{\cdot}0$
0	2·00	2·00	1·54	0·92	1·00	2·00
15	2·00	2·00	1·83	1·07	1·50	2·00
30	2·00	2·00	1·67	1·12	1·84	2·00
45	2·00	2·00	1·27	1·00	2·00	2·00

With the experimental data

Experimental data of Rowe & Davis[16,17] both in sands and clays were chosen for the comparison purpose.

Sands A series of model tests were conducted by Rowe & Davis[17] on the medium-grained quartz Sydney sand. For all the tests, the value of ϕ was in between 32–33.3°, and the value of dilatancy angle ψ was seen to vary from 4–10°. Test results with a length-to-breadth ratio equal to 8·75 were selected for the purpose of comparison so as to avoid any error due to the shape effect of anchors. Theoretical predictions were obtained by taking ϕ equal to 32·5°. The comparison of $p_u/(\gamma d)$ from the theory with the experimental data is shown in Figure 5. The theory provides a little higher

Table III. Comparison of F_q

	Uplift factor, F_q				
ϕ	Meyerhof and Adams [13]	Murray and Geddes [14]	Subba Rao and Kumar [19]	Present analysis, $m = 0{\cdot}5$	Present analysis, $m = 1{\cdot}0$
0	0·00	0·00	0·00	0·00	0·00
15	0·51	0·54	0·28	0·40	0·54
30	1·10	1·16	0·65	1·07	1·16
45	1·90	2·00	1·06	2·00	2·00

Table IV. Comparison of F_γ

	Uplift factor, F_γ					
ϕ	Meyerhof and Adams [13]	Murray and Geddes [14]	Rowe and Davis [17]	Subba Rao and Kumar [19]	Present analysis, $m = 0{\cdot}5$	Present analysis, $m = 1{\cdot}0$
0	0·00	0·00	0·00	0·00	0·00	0·00
15	0·26	0·27	0·28	0·21	0·21	0·27
30	0·55	0·58	0·63	0·41	0·54	0·58
45	0·95	1·00	1·18	0·50	1·00	1·00

values of failure loads in all the cases. The difference, however, is less than 20 per cent. The difference in the magnitudes of the failure loads obtained from the theory for $m = 0{\cdot}5$ and $1{\cdot}0$ is very marginal. It should be mentioned that the limit analysis is applicable for associated flow rule materials ($\psi = \phi$), whereas the selected experimental data are for non-associated flow rule ($\psi < \phi$). With the help of FEM analysis, Rowe and Davis has shown that the failure load increases with the increase in the dilatancy angle of the material.

Clays Anchor pullout tests in saturated Kaolin were conducted by Rowe and Davis[16]. In their experiments, the bond between the underside of the anchor and the clay was prevented by placing a filter paper under the surface of the anchor. This ensures that no contribution towards the pullout load arises from the soil lying below the anchor surface. Undrained condition ($\phi = 0°$) was maintained by loading the anchor very quickly. The clay was having an average undrained shear strength equal to 50 kPa. The value of $\gamma d/c$ for all the tests was less than 0·07. The comparison of p_u/c obtained from the theory for $\phi = 0°$ with the corresponding experimental data is shown in Figure 6. Experimental data in all the cases lie in between the corresponding theoretical values for $m = 0{\cdot}5$ and $1{\cdot}0$. The theory on the basis of $m = 1{\cdot}0$ provides larger pullout loads as compared to the experimental values.

CONCLUSIONS

The kinematic method of slices of Michalowski[11] has been used in this paper to obtain the upper bound on the ultimate uplift capacity of foundations. The effect of the yielding of soil mass with

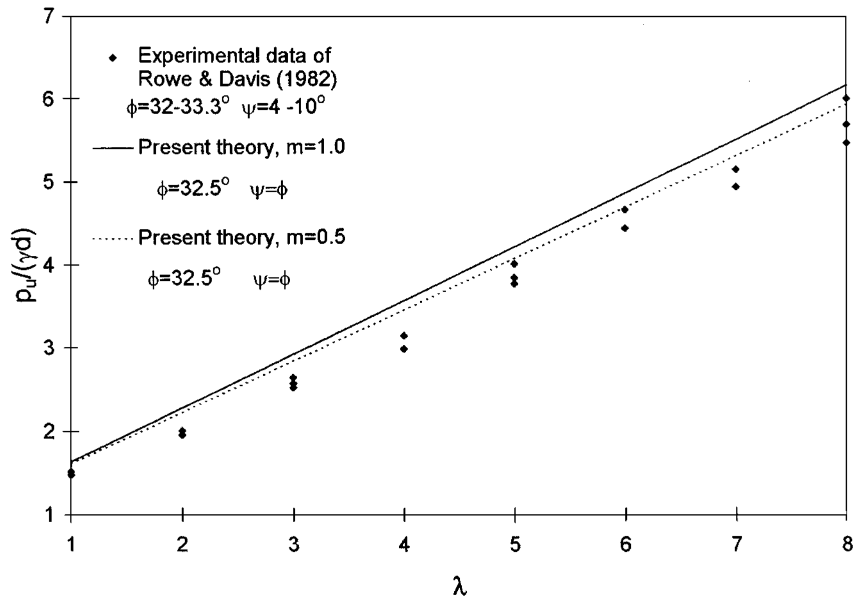

Figure 5. Comparison of the theory with the experimental data of Rowe and Davis[17] in sands

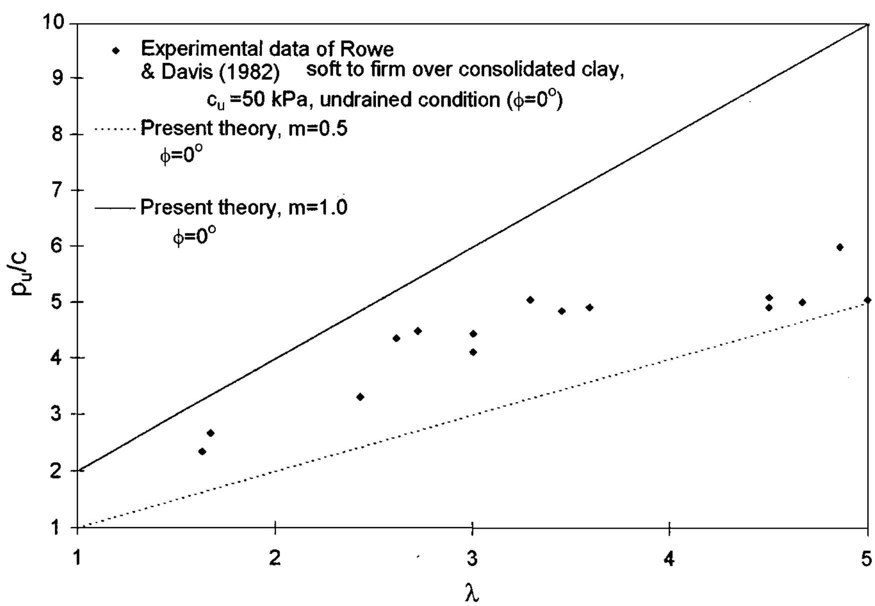

Figure 6. Comparison of the theory with the experimental data in Rowe and Davis[16] in clays

partial soil shear strength parameters along the interfaces of slices on the collapse load was investigated by introducing the soil strength factor m. The shape of the rupture surface remains curved for $m < 1$, but becomes linear for $m = 1$. The uplift capacity increases with the increase in the values of m. The results obtained compare reasonably well with the other existing theories as well as with the experimental tests data both in sands and clays.

REFERENCES

1. V. V. Sokolovoski, *Statics of Soil Media*, Butterworths Scientific Publication, England, 1960.
2. A. W. Bishop, 'The use of slip circle in the stability analysis of slopes', *Geotechnique*, **5**(1), 7–17 (1955).
3. N. Janbu, 'Earth pressure and bearing capacity calculations by generalised method of slices', *Proc*, *4th Int. Conf. Soil Mech. Found. Engng*., Vol. 2, London, 1957, pp. 207–212.
4. A. W. Bishop and N. R. Morgenstern, 'Slope stability coefficients for earth slopes', *Geotechnique*, **10**(4), 129–150 (1960).
5. N. R. Morgenstern and V. E. Price, 'The analysis of the stability of general slip surfaces', *Geotechnique*, **15**(1), 79–93 (1965).
6. E. Spencer, 'A method of analysis of the stability of embankments assuming parallel inter-slice forces', *Geotechnique*, **17**(1), 11–26 (1967).
7. J. Kumar and K. S. Subba Rao, 'Passive pressure determination by method of slices', *Int. J. Numer. Analyt. Meth. Geomech*., Vol. 21, USA, 1997, pp. 337–345.
8. W. F. Chen, *Limit Analysis and Soil Plasticity*, Elsevier, Amsterdam, 1975.
9. W. F. Chen and X. L. Liu, *Limit Analysis in Soil Mechanics* Elsevier, Amsterdam, 1990.
10. A. Drescher and E. Detournay, 'Limit load in translational materials for associated and non-associated materials', *Geotechnique*, **43**(3), 443–456 (1993).
11. R. L. Michalowski, 'Slope stability analysis: a kinematical approach', *Geotechnique*, **45**(2), 283–293 (1995).
12. J. Kumar and K. S. Subba Rao, 'Passive pressure coefficients, critical failure surface and its kinematic admissibility', *Geotechnique*, **47**(1), 185–192 (1997).
13. G. G. Meyerhof and S. I. Adams, 'The ultimate uplift capacity of foundations', *Canadian Geotech. J*., **5**(4), 225–244 (1968).
14. E. J. Murray and J. D. Geddes, 'Uplift of anchor plates in sand', *J. Geotech. Engng*., *ASCE*, **113**(3), 202–215 (1987).
15. J. Kumar, 'Upper bound solution for pullout capacity of anchors on sandy slopes', *Int. J. Numer. Analyt. Meth. Geomech*., **21**, 477–484 (1997).
16. R. K. Rowe and E. H. Davis, 'The behaviour of anchor plates in clay', *Geotechnique*, **32**(1), 9–23 (1982).
17. R. K. Rowe and E. H. Davis, 'The behaviour of anchor plates in sand', *Geotechnique*, **32**(1), 25–41 (1982).
18. J. Kumar, 'Theoretical Analyses of anchor pull-out capacity and associated earth pressure problems', *Ph.D. Thesis*, Indian Institute of Science, Bangalore, 1994.
19. K. S. Subba Rao and J. Kumar, 'Vertical uplift capacity of horizontal anchors', *J. Geotech. Engng. ASCE*, **120**(7), 1134–47 (1994).
20. M. Matsuo, 'Study on the uplift resistance of footings (I); *Soils and Foundations*, **7**(4), 1–37 (1967).
21. M. Matsuo, 'Study on the uplift resistance of footings (II); *Soils and Foundations*, **8**(1), 18–48 (1968).
22. K. Karal, 'Energy methods for slope stability problems', *J. Geotech. Engng. Div. ASCE*, **103**(5), 431–445 (1977).

